

## White matter alterations in anorexia nervosa: evidence from a voxel-based meta-analysis

Barona, Manuela<sup>1</sup>; Brown, Melanie<sup>2</sup>; Clark, Christopher<sup>1</sup>; Frangou, Sophia<sup>2</sup>; White, Tonya<sup>3</sup> & Micali, Nadia<sup>1,2,4\*</sup>.

<sup>1</sup> UCL Great Ormond Street Institute of Child Health, London, UK

<sup>2</sup> Department of Psychiatry, Icahn School of Medicine at Mount Sinai, New York, USA

<sup>3</sup> Department of Child and Adolescent Psychiatry/Psychology, Erasmus MC-Sophia Children's Hospital, Rotterdam, The Netherlands

<sup>4</sup> Department of Psychiatry, University of Geneva, Geneva Switzerland

**\*Corresponding author:** [nadia.micali@unige.ch](mailto:nadia.micali@unige.ch), Phone No: 0041 22 372 89 55

## **Abstract**

Anorexia nervosa (AN) is a severe psychiatric disorder with a complex and poorly understood etiology. Recent studies have sought to investigate differences in white matter microstructure in AN, with significant results in several brain regions. A systematic literature search of Embase, PubMed and Psychinfo databases was conducted in order to identify DTI studies of patients with AN and controls. We performed a meta-analysis of studies that met our inclusion criteria (N = 13) using effect size-signed differential mapping (AES-SDM) to detect differences in Fractional Anisotropy (FA) in patients with AN (N = 227) compared to healthy controls (N = 243). The quantitative meta-analysis of DTI studies identified decreased FA in the posterior areas of the corpus callosum, the left superior longitudinal fasciculus II, and the left precentral gyrus, as well as increased FA in the right cortico-spinal projections, and lingual gyrus in AN vs. controls. Studies of WM architecture are still limited in AN; further studies with longitudinal design are needed to better understand the complexity of abnormalities, and their persistence.

**Keywords:** eating disorders, anorexia nervosa, white matter, diffusion imaging, MRI, DTI

## Introduction

Anorexia Nervosa (AN) is a severe psychiatric disorder with a complex and poorly understood etiology and the highest mortality rate (12%) of any other psychiatric disorder (1). AN commonly begins during adolescence and affects mostly females (2); it is characterized by food restriction leading to low body weight, intense fear of gaining weight or persistent behavior that interferes with weight gain; and weight or shape concern, or persistent lack of recognition of the seriousness of the current low body weight (2). AN is not only a heterogeneous disorder with a complex multifactorial etiology, involving an interaction of neurobiological, psychological, and environmental mechanisms (3), but is further complicated by significant medical complications, including severe metabolic, electrolyte, and endocrine disturbances, as well as psychiatric comorbidity. Furthermore, it remains one of the most challenging psychiatric disorders to treat; especially in adults, with low rates of full recovery, about 25% of individuals develop a chronic course of illness (4).

In the last two decades, neuroimaging studies investigating brain structure and function in AN are beginning to provide valuable information on the neural correlates of the disorder. Recent systematic reviews have concluded that structural brain changes are frequently observed in patients with AN (5-8). AN has been associated with increased Cerebral Spinal Fluid (CSF) volume in the inter-hemispheric fissure, cortical sulci, and ventricles. In 2014 a meta-analysis by Seitz and colleagues (5) found that global grey matter (GM) was reduced by 5.6% on average in individuals with acute AN compared to healthy controls (HC) and global white matter (WM) was reduced by 3.7%, both in adults and adolescents with AN. Differences between groups after recovery (2 to 8 years) were no longer significant.

The heterogeneity of findings and large number of brain areas involved in the pathophysiology of eating disorders (ED) suggests a critical role of interconnections of cortical and subcortical regions, warranting therefore further exploration of WM structures in ED. Diffusion MRI allows the estimation of brain fiber structures using water diffusion properties as a proxy. Water molecules diffuse freely in a random manner (isotropic), however, in brain tissue water molecules diffuse more freely along the axon but are constrained from crossing the walls of the axon (anisotropic). Therefore, by calculating the diffusivity in multiple directions it is possible to estimate the directionality of axon bundles. Diffusion tensor imaging (DTI), a non-invasive magnetic resonance method based on the diffusion characteristics of water, has been used to study WM microstructure (9, 10). One of the most commonly used parameters for measuring WM microstructure is fractional anisotropy (FA), a scalar value that measures the directionality of water diffusion. To date, the large majority of DTI studies in AN have been based on small samples ( $n < 25$ ) and have mostly used voxel-based approaches to study water diffusion in the brain, with only three studies to date utilising tractography. As a recent review suggested however, results, have been mixed (see Monzon et. al. 2016 (11)). WM microstructure alterations have been found in acute patients with AN, both adults (12-19) and adolescents (19-24), in multiple WM tracts, including the fornix, cingulum, posterior thalamic-radiations, fronto-occipital fasciculus, superior longitudinal fasciculus, and cerebellum. Studies have also found abnormalities in recovered patients (13, 16, 17, 19). However, other studies have identified no differences in either acute or recovered patients vs. HC. Only three studies have used tractography to provide further details of WM microstructure. Travis and colleagues in 2015 (22) studied adolescents with acute AN and found both increased FA (in the thalamic radiation and left anterior longitudinal fasciculus) and decreased FA (in the fornix and

superior longitudinal fasciculus); whilst Hayes and colleagues in 2015(18) studied adults with acute AN who were treatment-resistant and found decreased FA in several areas including the fornix and cingulum. More recently Pfuhl and colleagues (25) found no differences in WM microstructure in acute or recovered patients with AN. Although most studies have found FA to be reduced, two studies, one by Frank and colleagues in 2013 (20) and a second by Vogel and colleagues in 2016 (21) reported an increase in FA (Vogel only reported increase while Frank and colleagues reported both increased and decreased FA), both studies only included adolescents. Available evidence therefore suggests that FA alterations are present in AN, however there is significant between-study variability as to the spatial distribution of these abnormalities making any conclusions on WM microstructure in patients with AN complex.

To our knowledge, no meta-analysis of studies of WM microstructure in AN has been carried out. Therefore, in the current study, we aimed to identify whether consistent changes in regional FA could be identified in AN patients compared to controls. To this purpose, we conducted a search of the available DTI literature in AN followed by a meta-analysis of eligible studies using anisotropic effect size-signed differential mapping (AES-SDM). As the most common methods used in the area of study are voxel-based methods, with only three tractography studies published to date, the meta-analysis will focus only on voxel-based methodology. We also performed a meta-regression to examine the mediating effect of Body Mass Index (BMI). Two exploratory subgroup analyses were also undertaken to determine the effect of age (studies including adults only) and stage of the disorder (studies focusing on subjects with acute illness ).

## **Methods and materials**

### *Data source*

We adhered to the guidelines detailed in the PRISMA Statement (26) and registered this study in PROSPERO (registration number CRD42016042525). A systematic and comprehensive search of databases, including Embase, PubMed and Psychinfo was carried out for studies published between January 1990 and May 2018. The search was performed using the following MESH terms and keywords: ('eating disorders' or 'anorexia nervosa' or 'AN' or 'anorexia') and ('dti' or 'diffusion tensor imaging' or 'diffusion weighted imaging' or 'tractography'). The search was finalized on the 1<sup>st</sup> May 2018.

### *Study selection*

Eligible DTI studies fulfilled the following inclusion criteria: (1) conducted voxel-based analyses; (2) compared FA values between AN and healthy controls; (3) reported whole-brain results in 3-dimensional coordinates (x, y, z); (4) used a threshold for significance and (5) were published in English.

Studies were excluded if: (1) tractography-based only study; (2) included eating disorders other than AN.

### *Quality assessment and data extraction*

Two authors independently screened, extracted and cross-checked the data from retrieved articles based on the eligibility criteria outlined above. The quality of the final studies was also independently checked by both authors using the Newcastle-Ottawa Scale (27) for assessing the quality of non-randomized studies in meta-analyses. For each study the following data were extracted: demographic information (age), sample size (sample size), age

(mean age), BMI (mean BMI), AN type and AN status (acute vs recovered) and the three-dimensional peak coordinates of case-control differences in each study.

### *Voxel-based meta-analysis*

A voxel-based meta-analysis of regional case-control differences in FA values of WM was performed using SDM software v4.31 (<http://www.sdmproject.com>) (28). The above method improves upon existing methods and has been used in several meta-analyses of voxel-based studies (29, 30). The software's main advantage is that it uses restricted maximum likelihood estimation of the variance with the reported peak coordinates to recreate maps of the positive and negative FA differences between patients and controls, rather than just assessing the probability or likelihood of a peak.

The method has three steps: (1) coordinates and magnitude of cluster peaks of case-control differences (e.g. the voxels where the differences between patients and health controls were highest in each study) are selected according to inclusion criteria, (2) the coordinates are used to recreate statistical maps, effect-size maps and their variances derived from t-statistics (Z- or p- values for significant clusters which were then converted to t-statistics using the SDM online conversion utilities), and (3) individual study maps are entered into the meta-analysis and the outcome is further tested in terms of sensitivity and heterogeneity.

In more detail, after the conversion of the coordinates to MNI space, an SDM map is created for each study using a specific mask (e.g. TBSS). The coordinates are then used to recreate statistical maps and effect sized maps. Pre-processing of reported peak coordinates (from each study) are done by recreating the clusters of difference by means on an anisotropic un-

normalized Gaussian Kernel, so that the voxels more correlated with the peak coordinate have effect-sizes similar to those of the peak. Finally, the resulting individual maps are meta-analyzed to complement the main outcome with sensitivity and heterogeneity analyses (The meta-analytic value of each voxel in the m-a map is defined as the proportion of studies reporting a coordinate around the voxel).

We first calculated the mean of the FA voxel peaks in the different studies, accounting for the variance and inter-study heterogeneity. A systematic whole-brain voxel-based jack-knife sensitivity analysis was performed using the leave-one out method. Exploratory subgroup analyses were also conducted to check for main differences based on age (adults vs. adolescents (under 18 years old) and illness status (acute vs. recovered).

The analytical parameters of SDM were those suggested by the software developers (28-31) and as follows: anisotropy = 1.0; isotropic full-width at half-maximum (FWHM) = 20 mm; voxel  $p = 0.005$ ; cluster = 10 voxels with 500 repetitions of standard randomization tests. A specific mask and correlation template for white matter was used. We used FSL visualization software (<http://fsl.fmrib.ox.ac.uk/fsl/fslwiki/>) to visualize SDM maps that were overlaid onto a high-resolution brain template (White matter atlas; <http://www.dtiatlas.org/>). An uncorrected  $p < 0.001$  was used, which has been described by the authors to be empirically equivalent to a corrected  $p < 0.05$ . All parameters were used as suggested by the authors of the meta-analytic method (28, 29, 31) and as previously used in other studies.

The coordinates for one of the main significant areas were extracted and separately mapped into a standard diffusion image to provide a three dimensional image of the most likely tracts



traversing a bounding 5mm box centred on the coordinates using MRtrix software (<http://www.mrtrix.org/>).

### *Meta-regression*

The effect of BMI was examined by means of simple linear regression, weighted by the square root of the sample size and restricted to only predict possible SDM values (i.e. from -1 to 1) in the observed range of values of the variable. The main output for each variable is a map of the regression slope. In order to minimize the detection of spurious relationships we decreased the probability threshold to 0.0005. Required abnormalities need to be detected both in the slope and in one of the extremes of the regressor. Findings in regions other than those detected in the main analyses were discarded. Further regression analyses were done using only adult and acute subgroups. Since the BMI used for adolescent samples was not standardized and a low BMI for adults could lie within the normal range for adolescents we run the regression analyses using the adult sample only. Meta-regression results should be taken with some caution because of the limited variability in the data and the low sample size.

## **Results**

The search strategy yielded a total of 387 studies, of which 13 met criteria for inclusion. The PRISMA diagram in Fig. 1 shows selection and exclusion of studies.

### *Meta-analysis: Included studies and sample characteristics*

Table 1 summarizes the characteristics of the 13 studies included in the meta-analysis. Table 2 summarizes the technical characteristics of studies included in the meta-analysis.

The included studies reported FA alterations of WM in individuals with AN (N = 227, mean age 22.5) relative to healthy controls (N = 243, mean age 21.9).

#### *Regional differences in FA*

MNI coordinates for the SDM meta-analysis were obtained from all 13 studies. As shown in table 3 and figure 2 and supplementary figure 1, patients with AN had significantly lower FA values in five clusters compared to healthy controls. Three of the five clusters exhibited a peak in the corpus callosum (CC) (MNI: -2,-18,18; 18,-58,30 and -22,24,30). The first peak (MNI = 2,-18,18) included voxels in the corpus callosum, thalamus, anterior thalamic projections, caudate nucleus, cortico-spinal projections and pons; the second peak (MNI = 18,-58,30) included voxels located in the corpus callosum, right precuneus and right cuneus and the third peak and smallest (MNI = -22,24,30) included voxels only in the corpus callosum. The two other peaks were found in the left superior longitudinal fasciculus II (MNI = -31,-34,36) and the left precentral gyrus, BA44 (MNI = -48,6,20). In addition, patients with AN had significantly higher FA values in the right cortico-spinal projections (MNI: 6,-16,-24), and right and left lingual gyrus BA18 (respectively: MNI = 10,-86,-12 and MNI = -28,-90,-14).

#### *Sensitivity analyses*

As shown in table 3, whole-brain jack-knife sensitivity analyses of the pooled meta-analysis indicated that FA reductions in AN patients vs. HC in the second and third cluster in the CC (respectively: MNI: 18,-58,30; MNI: -31,-34,36) were highly replicable; these findings were detected in ten out of the thirteen studies. Increased FA in the right cortico-spinal projections was present in only two of the thirteen studies.

As shown in supplementary figure 2, a funnel plot showed that all studies contributed to findings in the CC. Egger's test suggested no publication bias for these areas (Egger's  $p = 0.864$ ).

#### *Meta-regression*

BMI was not associated with AN-related FA reductions in any of the clusters across the combined or adult only sample.

BMI was associated with acute AN-related FA reductions in the cluster found in the Left precentral gyrus, BA 44 (MNI: (-48,6,20)).

#### *Subgroup analyses (individuals with acute AN and adults)*

As shown in table 4 and figures 3 and 4, the subgroup analyses revealed the following results.

Acute stage of illness (Table 4 and Figure 3): patients with active AN had both significantly lower and higher FA values in specific clusters when compared to healthy controls. There were five significant clusters of decreased FA: the first peak came up as undefined by the software (MNI = 2,-14,14), with voxels located in the corpus callosum, thalamus, anterior thalamic projections, pons, cortico spinal projections, right caudate nucleus and left superior longitudinal fasciculus. The second cluster was located in the corpus callosum (MNI = -22,24,30), the third cluster was located in the left precentral gyrus BA44 (MNI= -48,6,20), the fourth cluster was located in the left pons (MNI = -22,-14,-8) and the fifth cluster in the cingulum (MNI = 16,-56,28). In addition, acute patients also showed a number of small clusters of increased FA when compared to healthy controls (Table 4 and Figure 3).

Adults (Table 4 and figure 4): adult patients with AN had significantly lower FA values in two clusters when compared to adult healthy controls. The first cluster exhibited a peak in the right caudate nucleus (MNI: 16,2,24) and the second cluster exhibited a peak in the corpus callosum (18,-50,26).

## Discussion

This is the first meta-analysis comparing white matter microstructure in subjects with AN and healthy controls. We found that patients with AN had reduced FA in the CC, left SLF and precentral gyrus; and increased FA in the right-corticospinal projections, and lingual gyrus. The areas identified in the peri-splenial CC were robust and survived sensitivity analyses. FA reduction in the most posterior part of the CC survived sensitivity analyses in adult patients; this was also the case for the area identified in the precentral gyrus in the acute subgroup.

The CC is the largest WM tract containing more than 300 million axons connecting regions in both hemispheres and has been found to be critically involved in the integration of emotional, attentional, perceptual, and cognitive functions. The rostrum, genu, and rostral body of the CC contain fibres connecting homologous regions in the left and right prefrontal cortex; the midbody is formed by fibres connecting premotor, motor, and posterior parietal regions between the two hemispheres; and the splenium comprises connections between the superior and inferior temporal and occipital cortex (32). Based on our results, AN was associated with changes in the perisplenial CC, consistent with a tractography study by Travis et al. (22) which found FA reduction in patients with AN in subdivisions of the CC, including parietal, temporal and occipital projections.

Although the most robust peaks of case-control differences in the main analyses were located in the perisplenial CC (MNI = 18,-58,30; MNI = -22,24,30), the largest cluster (MNI = 18,-58,30), they extended to the right precuneus and right cuneus. We used MRtrix in order to identify the major tracts traversing this cluster (Supplementary Figure 1). The reduction in FA in these tracts would most likely impact the transfer of information between parietal and occipital regions and within the limbic system. Both structural and functional neuroimaging studies have consistently found the parietal cortex to be involved in AN (e.g. reduced GM and differential activation during tasks). This brain region is involved in the integration of proprioceptive and visual information of the body (33)(34). Furthermore, atypical patterns of activation in task fMRI studies have been found in areas of the occipitotemporal region (including the extrastriate body areas), and parietal cortex in patients with AN when observing digitally distorted images of their body (35, 36). Abnormal structural connectivity in these regions involved in body-image information processing might explain distorted body perception, a key feature in AN (2). Our findings also support the notion that parietal abnormalities in AN possibly lead to difficulties in haptic perception and spatial processing tasks (37, 38). Furthermore, two of the studies that did not meet criteria for inclusion in our meta-analysis found differences in areas associated with body self-image.

The largest cluster in the main analyses (MNI = -2,-18,18) was found in the CC as well, with most voxels located within the CC. However, there was involvement of other areas, including the anterior thalamic projections (ATR) and thalamus. A similar cluster, with involvement of the same areas (CC, thalamus and ATR) was found (although classified as undefined) in the acute subgroup. This is important as it could point to persistence of brain alterations

(following recovery) or to these differences being more stable markers of the disorder (biomarkers). However, it is also true that due to the nature of our analyses (with an heterogeneous sample) and the small sample, we are only able to propose this as a hypothesis. Due to the large number of studies of acutely ill subjects included in the main sample, it is also possible that these studies are driving the effect found in the main analyses. More studies are therefore needed in order to further elucidate this finding .

The ATR are fiber pathways that connect the anterior part of the thalamus with the frontal lobe, while the thalamus is part of a network that projects relevant sensory information to numerous brain areas (39) and also plays a role in higher-order cognition through relevant cortico-thalamic-cortical projections (40, 41). Cognitive behavioral inflexibility is an AN trait and has been conceptualized as impaired cognitive set shifting (rigid approaches to changing rules), and impaired behavioral response-shifting (perseverative behaviors). Numerous studies in the literature have found this trait in patients with AN, both ill and recovered as well as in healthy sisters (42). These findings suggest that impaired set shifting could be an endophenotype in AN (43). Our results of decreased FA in areas of the thalamus and anterior thalamic projections suggest a possible dysregulation in the pathways that project information relevant to set shifting and related behavioral response. In fact, areas of the fronto-striato-thalamic pathway have been found to be altered in patients with AN (44, 45).

A main finding is the cluster of reduced FA in the left precentral gyrus in an area also known as the pars opercularis of the inferior frontal gyrus, in Brodmann area 44. Although this cluster was the smallest in the main combined analyses, it was also found in the acute sample and was one of the most robust findings for this group. Furthermore, this cluster was found to be associated with BMI in the acute sample as well. This cluster is located in a motor area,

which lies in front of the central sulcus in the frontal lobe. Specifically the cluster was found in the Broadman area number 44 which has been recently found to be involved in suppression of response tendencies (46), such as during go-no-go tasks. Interestingly, the fact that this area was associated with BMI indicates that it is likely to be a result of the reduced weight during the acute stage of the disorder, rather than a more permanent marker of the disorder. However, this area was also found in the combined group analyses. One possible explanation is that this area is more affected than others by the low weight and the physiological aspects of AN, and might be a permanent scar of the disorder. However, we cannot disregard the possibility that differences in this area are present before the onset of the disorder and are further affected by it. Kothari and colleagues in 2013 (47) studied a large community sample of children at high risk for ED and found poorer behavioral inhibition in children of mothers with Bulimia Nervosa (BN), as well as a trend in children of mothers with AN. Therefore it is possible that alterations in this brain area already exist and become exacerbated during the acute stage of the disorder.

We did not find an association between BMI and FA in combined or adult samples. This is contrary to previous findings of a positive correlation between FA and current BMI in adult AN patients (12, 15, 17). However, in order to control for spurious results, the meta regression was limited to results found in the main areas reported in the meta-analysis, therefore, we can only conclude that there is no association in these areas. Studies have indeed reported associations with BMI involving regions which were not identified in this meta-analysis. Therefore, one possible explanation for this discrepancy is that FA decrements found are independent of low BMI and malnutrition, and a manifestation of trait abnormalities in AN. However, another possible explanation is that FA decrements in these

areas are secondary to malnutrition and do not recover with weight restoration. It is important to note that due to the small sample size of this meta-analysis, we cannot ensure that the lack of associations is due to methodological issues and not a real lack of association. Therefore, this requires further investigating in future meta-analyses.

The last major cluster of reduced FA in the main analysis was found in the SLF, a major intra-hemispheric fiber tract composed of four separate components. Our results show involvement of the left parietal part of SLF II, which occupies the central core of the WM above the insula, lateral to the corona radiata and CC (48). The SLF II fibers connect posterior parts of the superior temporal cortex with dorsolateral and ventrolateral prefrontal areas (48), and play a major role in visual and oculomotor aspects of spatial function (48). Similar to the area in the CC extending towards the precuneus, the SLF is functionally relevant to body image distortion in AN. The SLF II is the major WM tract connecting areas of important for body self-image (parietal), and body image perception (prefrontal and parietal network). The inferior parietal areas are involved in proprioception, spatial judgment and the integration of visual information, forming the neural basis for representation of body self-image (49). Several studies have found differences in parietal areas in patients with AN as well as in prefrontal areas during visualization of own body image during fMRI studies (49).

As well as areas identified in the main meta-analysis, a cluster of decreased FA was found in the pons only in the acute group. The pons connects the limbic forebrain and brainstem and is vital to autonomic functions necessary for life, including food pleasure (50). Areas in the pons and thalamus receive information from the lower brainstem in relation to the properties of food and project to the amygdala and frontal cortex, which perform higher



order functions pertaining to the rewarding and aversive aspects of food. Thus, alterations in pontine white matter could disrupt the food reward system, which has been shown to be altered in eating disorders (50, 51). Malnutrition during the acute phases of the illness may contribute to persistent reduction in FA in the pons in AN. This possibility is supported by reports of central pontine myelinolysis (CPM) in AN (52-54); this is a demyelinating lesion in the pons that was first reported in cases of malnutrition and alcoholism. Since decreased FA only appeared in subgroup acute analysis, it is possible that alterations found in the pons are due to malnutrition.

Analyses in adult patients only implicated the right caudate nucleus and the most robust area in the CC. The caudate nucleus is one of the structures that makes up the dorsal striatum, a component of the basal ganglia. This area has shown to be involved in several roles, including executive functions (55, 56) (especially inhibitory control and planning) and it has been shown to also play a role in the reward system as part of the cortico-basal ganglia-thalamic loop. The basal ganglia are important in disorders such as obsessive compulsive disorder (OCD) and attention-deficit/hyperactivity disorder (ADHD), which are often comorbid with ED (57).

Finally, one small cluster of decreased FA in the cingulum was found in the acute subgroup and showed involvement of the CC as well. The cingulum is a projection of white matter fibers that allow communication between components of the limbic system and that is located adjacent to the CC. The area of decreased FA was found in the middle towards the anterior part of the cingulum. The anterior part of the cingulum has been linked with emotion, motivation and executive functions (58). Alterations in this structure have been

found to be associated with altered emotion identification in AN, as well as difficulties with cognitive control.

Both the main analyses and acute ones found areas of increased FA, however, these results should be taken with some caution as they were driven by results in adolescent studies and therefore disappeared when analyzing adult groups only. Three out of the four studies on adolescents found increased FA and were therefore driving the findings of increased FA. Furthermore, results only show small sized clusters (less than 100 voxels) compared to those found for decreased FA. In the combined analyses, only three clusters of increased FA were found, however, the acute subgroup had a larger and more widespread number of increased FA clusters. Only nine studies were included in the acute sample and three of those were the studies on adolescents with increased FA, therefore it is likely that these studies had more weight in this analyses than they did in the combined ones (where 13 studies were included).

The first cluster found in both the combined and acute sample analyses is located in the corticospinal projections. Interestingly, to date, studies on white matter microstructure in adolescents with AN have found mixed results, with some brain regions showing increased FA and others showing decreased FA compared to controls. Differences in the direction (increased rather than decreased) of FA might be due to an unmasking effect. The corticospinal tract has significant crossing fibres, therefore, if one of these pathways has low FA this might result in a higher FA overall. Interestingly, in the cluster breakdown of the largest peak of decreased FA, some voxels were located in the cortico spinal projections. However, it is important to note that there are only four studies investigating adolescent

samples published to date, and therefore more studies are needed in order to understand the differences between adolescent and adult samples.

The two most robust findings of increased FA in the acute sample were found in the putamen and the arcuate network. The putamen is a structure located at the base of the forebrain and together with the caudate nucleus it forms the dorsal striatum which is one of the structures that composes the basal ganglia. Alterations in the dorsal striatum are of interest to ED as they have been shown to play a role in supporting rewarding behaviors based on previous experience (59). Dorsal striatum responds to reward and punishment and contributes to reward based decision making (60). Although the results show increased FA, it could still reflect damage as increased tissue anisotropy of the basal ganglia is thought to reflect microstructural GM damage (61, 62). These results would therefore support those found by Frank and colleagues (63), who found alterations in GM in the putamen which predicted sensitivity to reward. Therefore, alterations in the putamen could therefore play a role in differences in sensitivity to punishment and reward found in patients with AN (64).

An undefined area with voxels mostly in the cerebellum was also a replicable finding of increased FA. Findings in the cerebellum are of interest for the pathophysiology of AN due to the role it plays in feeding behavior. The cerebellum connects to the hypothalamus through cerebello-hypothalamic circuits which are thought to be involved in the regulation of food intake and feelings of satiety (65). Studies have also focused on the role that the cerebellum plays in cognition and emotional experience (66) which again is of interest for the development and maintenance of AN. Volumetric reductions in cerebellar GM have been found in patients with AN (67) as well as deficits in functions associated to the cerebellum.

This meta-analysis found increased FA in this area, however, because FA is sensitive to several tissue characteristics, it needs to be interpreted carefully, a range of tissue characteristics might change in such a way that the resulting FA obscures subtle changes. More research is needed to further understand alterations in the cerebellum and the direction as well as associations with deficits in AN.

The cross-sectional design of the available studies does not address the issue of causality and specifically the contribution of nutritional status. GM and WM volumes can show significant reductions in otherwise psychiatrically healthy individuals after only 2-3 days of dehydration (68) and WM volumes can be restored following re-feeding. Furthermore, a commentary by Frank in 2015 (69) discussed the variance in time between start of re-alimentation and scanning as another point of variability that might account for differences between structural MRI studies in AN. In fact, the studies included in the meta-analysis show a degree of variance with regards to this issue, whilst six of the ten studies of acute patients (12,14,15,20) controlled for the effect of re-feeding in some respect, most of them scanned patients after one to two weeks of rehydration. However, it is not known whether more subtle WM differences persist over time following recovery. Axons in the corticospinal tracts and the corpus callosum are some of the largest axons in the brain (51) and therefore have thicker myelin and larger concentrations of lipids (70). As such, these areas could be predisposed to greater degree of myelin loss secondary to malnutrition or chronicity.

Whilst this meta-analysis sheds some light into what could be more stable WM microstructure alterations in AN, it does not help elucidate if these alterations are a cause or a consequence of the disorder. Although subgroup analyses are exploratory because of the

sample size, there are differences in the number of areas found between the main analysis (which include both acute and recovered) and the acute group only, with the second subgroup analysis finding a larger number of areas different in AN vs HC. One possible explanation for this is that in the acute stage, patients have a more widespread number of white matter micro-structural abnormalities, and that one year after recovery (criteria for inclusion in both studies with recovered patients) only some differences persist. These differences could either be more permanent scars of the disorder or could possibly be present before the onset and therefore contribute to the development of the disorder. To date, four studies have investigated recovered patients, however, only three met criteria for inclusion in this meta-analysis and therefore we were not able to run subgroup analyses. Taken together, these four studies (13, 16, 17, 19) showed inconsistencies in WM integrity abnormalities identified, with two studies finding decreased FA, one finding increased FA and one only finding decreased MD. It is important to note that not all studies use the same criteria for recovery making comparability of the results complex. However, the studies included in the meta-analysis used a 1-year criterion of weight restoration and no engagement in ED behaviors for their recovered patients. Only one of the studies had short recovery criteria, i.e. weight restoration only for two weeks (19). Although this study was included in the meta analysis, whole brain white matter differences were only reported during the acute period and not in the second stage after weight restoration. Of the studies with more stringent recovery criteria (one year recovery and no ED behaviors), two did not find any differences in FA, however, these studies only included nine and twelve recovered patients, while the study by Shott and colleagues (16) included 24 patients ensuring increased power for their analyses. Importantly, more studies with recovered patients are needed to ascertain if differences do persist after recovery, or if WM alterations are a

temporary scar of the disorder. Furthermore, although, methodological differences in the studies could account for some variability in results, they are unlikely to account for differences in the direction of DTI parameter changes. Taken together, these studies suggest that some FA alterations may be present in weight recovered patients but also that WM integrity and myelin may be improved with weight restoration in AN in some brain areas. It is unclear whether the differences found in recovered patients are an antecedent or a scar of the disorder (related to severity of illness or specific symptoms), and/or an artefact of heterogeneous methodology employed to measure WM integrity. Importantly, there is a need for longitudinal prospective studies investigating an at-risk population that will allow us to investigate differences before the onset of the disorder.

### *Limitations*

Overall, results from DTI studies should be taken with caution as there are some limitations that should be acknowledged. One of the most common issues with DTI is data interpretation, usually higher MD and lower FA indicate damaged or impaired fiber integrity due to increased diffusion and loss of coherence in movement direction. However, this is not always true, and it can be dependent on brain region, cellular basis, or the sample studied. Studies in patients with schizophrenia have shown an overall reduction of FA, however, increased FA (71) has been found in interhemispheric auditory fibers in those patients suffering from hallucinations. Therefore, it cannot be said that increased FA is always better. Another potential limitation involves the questions of how much FA abnormalities truly reflect altered WM integrity. Usually, FA is described as a marker of WM integrity, however it can be altered due to a variety of reasons (72, 73), such as larger axon diameter and lower packing density of fibers (both contributing to fewer barriers to diffusion leading to lower

FA), or increased membrane permeability and reduced myelination.(73) Crossing fibers (previously discussed in this section) are also problematic in DTI result interpretation. A single voxel can be composed by fiber populations with different spatial orientation which can result in an average increase in FA, however, in this case, this is not due to changes in axonal or myelin structure.

The present meta-analysis has several limitations. First, the number of studies utilizing DTI in AN is rather small, and not all studies of AN could be included due to methodological differences, therefore the results are preliminary and further meta-analyses are necessary as studies continue to be published. Second, although the meta-analytic methods used provide good control of false positive results, they do not for false negative results (31). Third, the studies included in this meta-analysis used different statistical thresholds. However, although thresholds involving correction for multiple corrections are desired, it is still statistically correct to include those studies using more liberal thresholds (31). Fourth, the heterogeneity of the MRI acquisition, including differences in acquisition parameters and the use of two different methods (TBSS and VBA) to undertake whole brain analysis may lead to inconsistencies between studies. However, these limitations are inherent to all meta-analyses and in spite of them, some findings were quite robust. Meta-analysis combining TBSS and VBA analysis have been published including a study by the developers of the software. As published in the supplementary methods, to allow combinations of VBA and TBSS studies the TBSS template included in AES-SDM was adopted. Fifth, the studies varied in terms of patient characteristics, not only in terms of illness status (acute and recovered) and duration of illness, but also for the inclusion of both binge/purge and restricting types of AN. As further studies are published, future meta-analytic studies should subcategorize between types of

AN in order to ascertain neural differences between both binge/purge and restricting AN as well as different stages of illness duration. Sixth, the main finding in this meta-analysis involves a cluster of voxels in the CC, however, Figure 2 shows how these areas surround ventricular areas. Although the image is just a rough illustration of the location, it is worth noting that since ventricles are enlarged in AN, a biased estimation of FA in these areas can be due to partial volumes effects (74). Finally, this meta-analysis only focused on FA as it is the most commonly reported variable to show differences in WM microstructure (both in the wider literature and in the studies included in this meta-analysis).

### *Conclusions*

In conclusion, by summarizing WM microarchitecture studies to date, we have demonstrated significant FA alterations in patients with AN, affecting white matter tracts in the CC and in subcortical regions. This evidence implicates regions likely to be involved in body image processing and cognitive behavioral inflexibility. Further studies are needed to examine the direction of causality of these findings. These results integrate previous findings from DTI studies in AN and provide a more coherent picture of the most prominent and replicable abnormalities in WM integrity in patients with AN.

### **Acknowledgments**

This study was supported by a 'NARSAD independent investigator' award from the Brain and Behavior Research Foundation to Dr. Micali, a grant from Swiss Anorexia Nervosa Foundation, and a small grant from the Rosetrees Trust.

### **Financial Disclosures**



No financial or non-financial conflicts of interest exist for any of the authors.

## References

1. Arcelus J, Mitchell AJ, Wales J, Nielsen S. Mortality rates in patients with anorexia nervosa and other eating disorders: A meta-analysis of 36 studies. *Archives of General Psychiatry*. 2011;68(7):724-31.
2. APA. *Diagnostic and Statistical Manual of Mental Disorders (DSM-5®)*: American Psychiatric Pub; 2013.
3. Bulik CM. Exploring the gene-environment nexus in eating disorders. *Journal of psychiatry & neuroscience : JPN*. 2005;30(5):335-9.
4. Berkman ND, Lohr KN, Bulik CM. Outcomes of eating disorders: A systematic review of the literature. *International Journal of Eating Disorders*. 2007;40(4):293-309.
5. Seitz J, Buhren K, Von Polier GG, Heussen N, Herpertz-Dahlmann B, Konrad K. Morphological changes in the brain of acutely ill and weight-recovered patients with anorexia nervosa: A meta-analysis and qualitative review. [German, English]. *Zeitschrift fur Kinder- und Jugendpsychiatrie und Psychotherapie*. 2014;42(1):7-18.
6. Phillipou A, Rossell SL, Castle DJ. The neurobiology of anorexia nervosa: a systematic review. *The Australian and New Zealand journal of psychiatry*. 2014;48(2):128-52.
7. Van den Eynde F, Suda M, Broadbent H, Guillaume S, Van den Eynde M, Steiger H, et al. Structural Magnetic Resonance Imaging in Eating Disorders: A Systematic Review of Voxel-Based Morphometry Studies. *European Eating Disorders Review*. 2012;20(2):94-105.
8. Titova OE, Hjorth OC, Schioth HB, Brooks SJ. Anorexia nervosa is linked to reduced brain structure in reward and somatosensory regions: A meta-analysis of VBM studies. *BMC Psychiatry*. 2013;13 (no pagination)(110).
9. Le Bihan D, Johansen-Berg H. Diffusion MRI at 25: exploring brain tissue structure and function. *Neuroimage*. 2012;61(2):324-41.
10. Beaulieu C. The basis of anisotropic water diffusion in the nervous system - a technical review. *NMR Biomed*. 2002;15(7-8):435-55.
11. Martin Monzon B, Hay P, Foroughi N, Touyz S. White matter alterations in anorexia nervosa: A systematic review of diffusion tensor imaging studies. *World J Psychiatry*. 2016;6(1):177-86.
12. Kazlouski D, Rollin MD, Tregellas J, Shott ME, Jappe LM, Hagman JO, et al. Altered fimbria-fornix white matter integrity in anorexia nervosa predicts harm avoidance. *Psychiatry Res*. 2011;192(2):109-16.

13. Frieling H, Fischer J, Wilhelm J, Engelhorn T, Bleich S, Hillemacher T, et al. Microstructural abnormalities of the posterior thalamic radiation and the mediodorsal thalamic nuclei in females with anorexia nervosa--a voxel based diffusion tensor imaging (DTI) study. *Journal of psychiatric research*. 2012;46(9):1237-42.
14. Via E, Zalesky A, Sanchez I, Forcano L, Harrison BJ, Pujol J, et al. Disruption of brain white matter microstructure in women with anorexia nervosa. *Journal of psychiatry & neuroscience : JPN*. 2014;39(6):367-75.
15. Nagahara Y, Nakamae T, Nishizawa S, Mizuhara Y, Moritoki Y, Wada Y, et al. A tract-based spatial statistics study in anorexia nervosa: abnormality in the fornix and the cerebellum. *Progress in neuro-psychopharmacology & biological psychiatry*. 2014;51:72-7.
16. Shott ME, Pryor TL, Yang TT, Frank GKW. Greater Insula White Matter Fiber Connectivity in Women Recovered from Anorexia Nervosa. *Neuropsychopharmacology : official publication of the American College of Neuropsychopharmacology*. 2016;41(2):498-507.
17. Yau W-YW, Bischoff-Grethe A, Theilmann RJ, Torres L, Wagner A, Kaye WH, et al. Alterations in white matter microstructure in women recovered from anorexia nervosa. *International Journal of Eating Disorders*. 2013;46(7):701-8.
18. Hayes DJ, Lipsman N, Chen DQ, Woodside DB, Davis KD, Lozano AM, et al. Subcallosal Cingulate Connectivity in Anorexia Nervosa Patients Differs From Healthy Controls: A Multi-tensor Tractography Study. *Brain stimulation*. 2015;8(4):758-68.
19. Cha J, Ide JS, Bowman FD, Simpson HB, Posner J, Steinglass JE. Abnormal reward circuitry in anorexia nervosa: A longitudinal, multimodal MRI study. *Hum Brain Mapp*. 2016.
20. Frank GK, Shott ME, Hagman JO, Yang TT. Localized brain volume and white matter integrity alterations in adolescent anorexia nervosa. *Journal of the American Academy of Child and Adolescent Psychiatry*. 2013;52(10):1066-75.
21. Vogel K, Timmers I, Kumar V, Nickl-Jockschat T, Bastiani M, Roebroek A, et al. White matter microstructural changes in adolescent anorexia nervosa including an exploratory longitudinal study. *NeuroImage : Clinical*. 2016;11:614-21.
22. Travis KE, Golden NH, Feldman HM, Solomon M, Nguyen J, Mezer A, et al. Abnormal white matter properties in adolescent girls with anorexia nervosa. *Neuroimage Clin*. 2015;9:648-59.
23. Gaudio S, Quattrocchi CC, Piervincenzi C, Zobel BB, Montecchi FR, Dakanalis A, et al. White matter abnormalities in treatment-naive adolescents at the earliest stages of Anorexia Nervosa: A diffusion tensor imaging study. *Psychiatry Res Neuroimaging*. 2017;266:138-45.
24. Hu SH, Feng H, Xu TT, Zhang HR, Zhao ZY, Lai JB, et al. Altered microstructure of brain white matter in females with anorexia nervosa: a diffusion tensor imaging study. *Neuropsychiatr Dis Treat*. 2017;13:2829-36.
25. Pfuhl G, King JA, Geisler D, Roschinski B, Ritschel F, Seidel M, et al. Preserved white matter microstructure in young patients with anorexia nervosa? *Human Brain Mapping*. 2016:No Pagination Specified.
26. Moher D, Liberati A, Tetzlaff J, Altman DG. Preferred reporting items for systematic reviews and meta-analyses: the PRISMA statement. *BMJ*. 2009;339.
27. Wells G, Shea B, O'Connell D, Peterson J, Welch V, Losos M, et al. The Newcastle-Ottawa Scale (NOS) for assessing the quality if nonrandomized studies in meta-analyses [Available from: [http://www.ohri.ca/programs/clinical\\_epidemiology/oxford.htm](http://www.ohri.ca/programs/clinical_epidemiology/oxford.htm)].
28. Radua J, Mataix-Cols D. Voxel-wise meta-analysis of grey matter changes in obsessive-compulsive disorder. *Br J Psychiatry*. 2009;195(5):393-402.
29. Radua J, Via E, Catani M, Mataix-Cols D. Voxel-based meta-analysis of regional white-matter volume differences in autism spectrum disorder versus healthy controls. *Psychol Med*. 2011;41(7):1539-50.
30. Bora E, Fornito A, Yücel M, Pantelis C. Voxelwise Meta-Analysis of Gray Matter Abnormalities in Bipolar Disorder. *Biological Psychiatry*. 2010;67(11):1097-105.

31. Radua J, Mataix-Cols D, Phillips ML, El-Hage W, Kronhaus DM, Cardoner N, et al. A new meta-analytic method for neuroimaging studies that combines reported peak coordinates and statistical parametric maps. *Eur Psychiatry*. 2012;27(8):605-11.
32. Hofer S, Frahm J. Topography of the human corpus callosum revisited—Comprehensive fiber tractography using diffusion tensor magnetic resonance imaging. *NeuroImage*. 2006;32(3):989-94.
33. Shimada S, Hiraki K, Oda I. The parietal role in the sense of self-ownership with temporal discrepancy between visual and proprioceptive feedbacks. *Neuroimage*. 2005;24(4):1225-32.
34. Zhang HW, Li DY, Zhao J, Guan YH, Sun BM, Zuo CT. Metabolic imaging of deep brain stimulation in anorexia nervosa: a 18F-FDG PET/CT study. *Clinical nuclear medicine*. 2013;38(12):943-8.
35. Uher R, Murphy T, Friederich H-C, Dalglish T, Brammer MJ, Giampietro V, et al. Functional neuroanatomy of body shape perception in healthy and eating-disordered women. *Biological psychiatry*. 2005;58(12):990-7.
36. Grönemeyer D, Herpertz S. Neural correlates of viewing photographs of one's own body and another woman's body in anorexia and bulimia nervosa: an fMRI study. *Journal of psychiatry & neuroscience: JPN*. 2010;35(3):163.
37. Grunwald M, Ettrich C, Busse F, Assmann B, Dähne A, Gertz H. Angle paradigm: a new method to measure right parietal dysfunctions in anorexia nervosa. *Arch Clin Neuropsychol*. 2002;17.
38. Grunwald M, Ettrich C, Assmann B, Dähne A, Krause W, Busse F, et al. Deficits in haptic perception and right parietal theta power changes in patients with anorexia nervosa before and after weight gain. *Int J Eat Disord*. 2001;29.
39. Fan J, McCandliss BD, Fossella J, Flombaum JI, Posner MI. The activation of attentional networks. *Neuroimage*. 2005;26(2):471-9.
40. Sherman SM. The thalamus is more than just a relay. *Curr Opin Neurobiol*. 2007;17(4):417-22.
41. Klostermann F, Wahl M, Marzinzik F, Schneider GH, Kupsch A, Curio G. Mental chronometry of target detection: human thalamus leads cortex. *Brain*. 2006;129(Pt 4):923-31.
42. Roberts ME, Tchanturia K, Stahl D, Southgate L, Treasure J. A systematic review and meta-analysis of set shifting ability in eating disorders. *Psychol Med*. 2007;37.
43. Holliday J, Tchanturia K, Landau S, Collier DA, Treasure J. Is impaired set-shifting an endophenotype of anorexia nervosa? *Am J Psychiatry*. 2005;162.
44. Zastrow A, Kaiser S, Stippich C, Walther S, Herzog W, Tchanturia K, et al. Neural correlates of impaired cognitive-behavioral flexibility in anorexia nervosa. *Am J Psychiatry*. 2009;166(5):608-16.
45. Shafritz KM, Kartheiser P, Belger A. Dissociation of neural systems mediating shifts in behavioral response and cognitive set. *Neuroimage*. 2005;25(2):600-6.
46. Forstmann BU, van den Wildenberg WP, Ridderinkhof KR. Neural mechanisms, temporal dynamics, and individual differences in interference control. *J Cogn Neurosci*. 2008;20(10):1854-65.
47. Kothari R, Solmi F, Treasure J, Micali N. The neuropsychological profile of children at high risk of developing an eating disorder. *Psychol Med*. 2013;43(7):1543-54.
48. Makris N, Kennedy DN, McInerney S, Sorensen AG, Wang R, Caviness VS, et al. Segmentation of subcomponents within the superior longitudinal fascicle in humans: a quantitative, in vivo, DT-MRI study. *Cereb Cortex*. 2005;15(6):854-69.
49. Gaudio S, Quattrocchi CC. Neural basis of a multidimensional model of body image distortion in anorexia nervosa. *Neurosci Biobehav Rev*. 2012;36(8):1839-47.
50. Berridge KC. 'Liking' and 'wanting' food rewards: Brain substrates and roles in eating disorders. *Physiology & behavior*. 2009;97(5):537-50.
51. Lassek AM. The human pyramidal tract. IV. A study of the mature, myelinated fibers of the pyramid. *The Journal of Comparative Neurology*. 1942;76(2):217-25.
52. Keswani SC. Central pontine myelinolysis associated with hypokalaemia in anorexia nervosa. *J Neurol Neurosurg Psychiatry*. 2004;75(4):663; author reply

53. Amann B, Schäfer M, Sterr A, Arnold S, Grunze H. Central pontine myelinolysis in a patient with anorexia nervosa. *Int J Eat Disord*. 2001;30(4):462-6.
54. Ramírez N, Arranz B, Martín C, San L. [Course and prognosis of a case of central pontine myelinolysis in eating behavior disorder]. *Actas Esp Psiquiatr*. 2007;35(2):141-4.
55. Grahn JA, Parkinson JA, Owen AM. The cognitive functions of the caudate nucleus. *Progress in Neurobiology*. 2008;86(3):141-55.
56. Villablanca JR. Why do we have a caudate nucleus? *Acta neurobiologiae experimentalis*. 2010;70(1):95-105.
57. Murphy DL, Timpano KR, Wheaton MG, Greenberg BD, Miguel EC. Obsessive-compulsive disorder and its related disorders: a reappraisal of obsessive-compulsive spectrum concepts. *Dialogues in clinical neuroscience*. 2010;12(2):131-48.
58. Bubb EJ, Metzler-Baddeley C, Aggleton JP. The cingulum bundle: Anatomy, function, and dysfunction. *Neurosci Biobehav Rev*. 2018;92:104-27.
59. O'Doherty J, Dayan P, Schultz J, Deichmann R, Friston K, Dolan RJ. Dissociable roles of ventral and dorsal striatum in instrumental conditioning. *Science*. 2004;304(5669):452-4.
60. Balleine BW, Delgado MR, Hikosaka O. The role of the dorsal striatum in reward and decision-making. *J Neurosci*. 2007;27(31):8161-5.
61. Hannoun S, Durand-Dubief F, Confavreux C, Ibarrola D, Streichenberger N, Cotton F, et al. Diffusion tensor-MRI evidence for extra-axonal neuronal degeneration in caudate and thalamic nuclei of patients with multiple sclerosis. *AJNR Am J Neuroradiol*. 2012;33(7):1363-8.
62. Cavallari M, Ceccarelli A, Wang GY, Moscufo N, Hannoun S, Matulis CR, et al. Microstructural changes in the striatum and their impact on motor and neuropsychological performance in patients with multiple sclerosis. *PLoS One*. 2014;9(7):e101199.
63. Frank GK, Shott ME, Hagman JO, Mittal VA. Alterations in brain structures related to taste reward circuitry in ill and recovered anorexia nervosa and in bulimia nervosa. *American Journal of Psychiatry*. 2013;170(10):1152-60.
64. Harrison A, O'Brien N, Lopez C, Treasure J. Sensitivity to reward and punishment in eating disorders. *Psychiatry Res*. 2010;177(1-2):1-11.
65. Zhu JN, Wang JJ. The cerebellum in feeding control: possible function and mechanism. *Cell Mol Neurobiol*. 2008;28(4):469-78.
66. Stoodley CJ, Schmahmann JD. Functional topography in the human cerebellum: a meta-analysis of neuroimaging studies. *Neuroimage*. 2009;44(2):489-501.
67. Boghi A, Sterpone S, Sales S, D'Agata F, Bradac GB, Zullo G, et al. In vivo evidence of global and focal brain alterations in anorexia nervosa. *Psychiatry Research - Neuroimaging*. 2011;192(3):154-9.
68. Streitburger DP, Moller HE, Tittgemeyer M, Hund-Georgiadis M, Schroeter ML, Mueller K. Investigating structural brain changes of dehydration using voxel-based morphometry. *PLoS One*. 2012;7(8):e44195.
69. Frank GK. Advances from neuroimaging studies in eating disorders. *CNS Spectr*. 2015;20(4):391-400.
70. Paus T. Growth of white matter in the adolescent brain: myelin or axon? *Brain and cognition*. 2010;72(1):26-35.
71. Kubicki M, McCarley R, Westin CF, Park HJ, Maier S, Kikinis R, et al. A review of diffusion tensor imaging studies in schizophrenia. *J Psychiatr Res*. 2007;41(1-2):15-30.
72. Jones DK, Leemans A. Diffusion tensor imaging. *Methods Mol Biol*. 2011;711:127-44.
73. Jones DK, Knösche TR, Turner R. White matter integrity, fiber count, and other fallacies: the do's and don'ts of diffusion MRI. *Neuroimage*. 2013;73:239-54.
74. Jones DK, Cercignani M. Twenty-five pitfalls in the analysis of diffusion MRI data. *NMR Biomed*. 2010;23(7):803-20.

75. Bang L, Rø Ø, Endestad T. Normal white matter microstructure in women long-term recovered from anorexia nervosa: A diffusion tensor imaging study. *Int J Eat Disord.* 2018;51(1):46-52.
76. Olivo G, Wiemerslage L, Swenne I, Zhukowsky C, Salonen-Ros H, Larsson EM, et al. Limbic-thalamo-cortical projections and reward-related circuitry integrity affects eating behavior: A longitudinal DTI study in adolescents with restrictive eating disorders. *PLoS One.* 2017;12(3):e0172129.

Figure 1. Flow diagram for the identification and exclusion of studies.

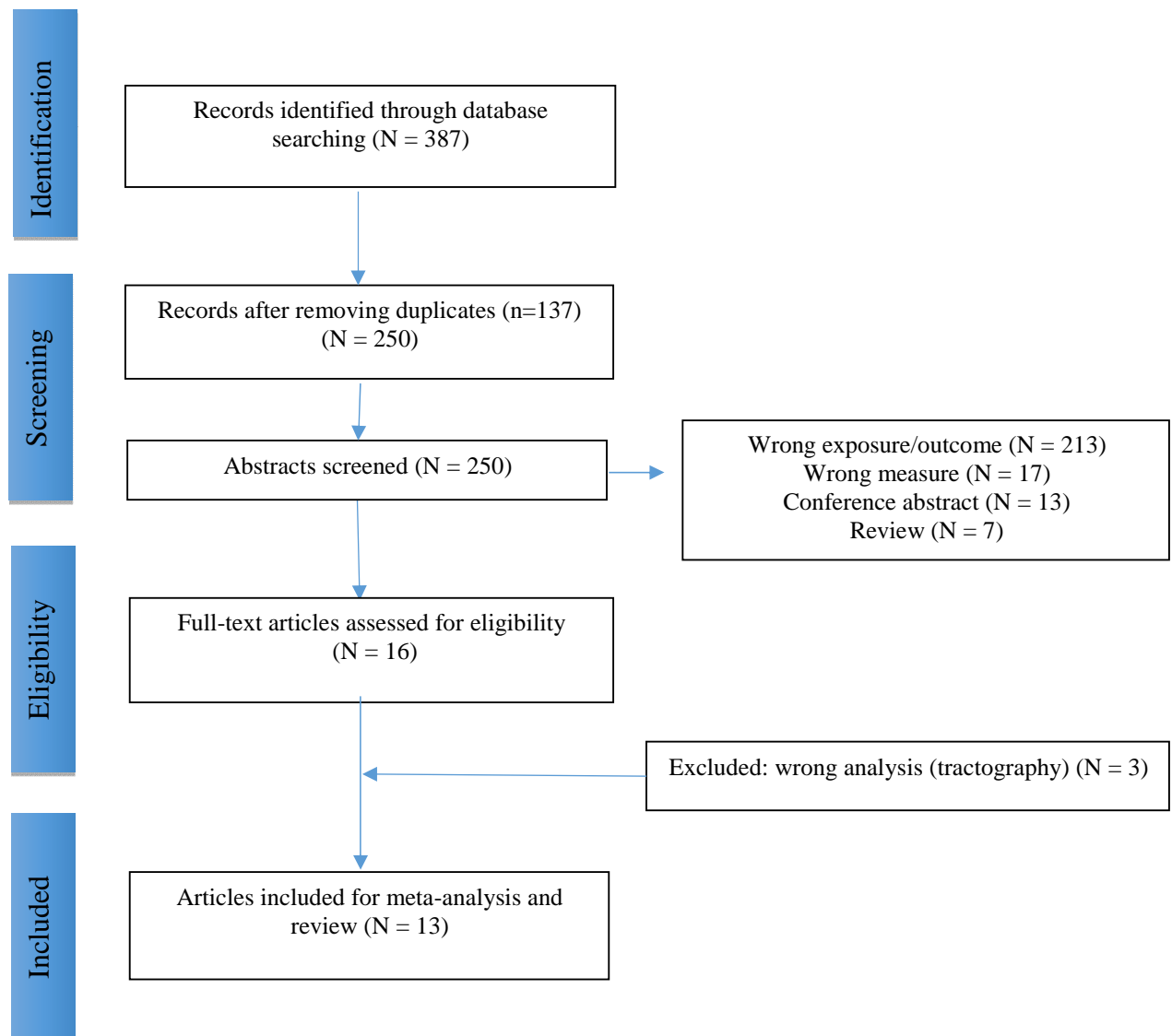
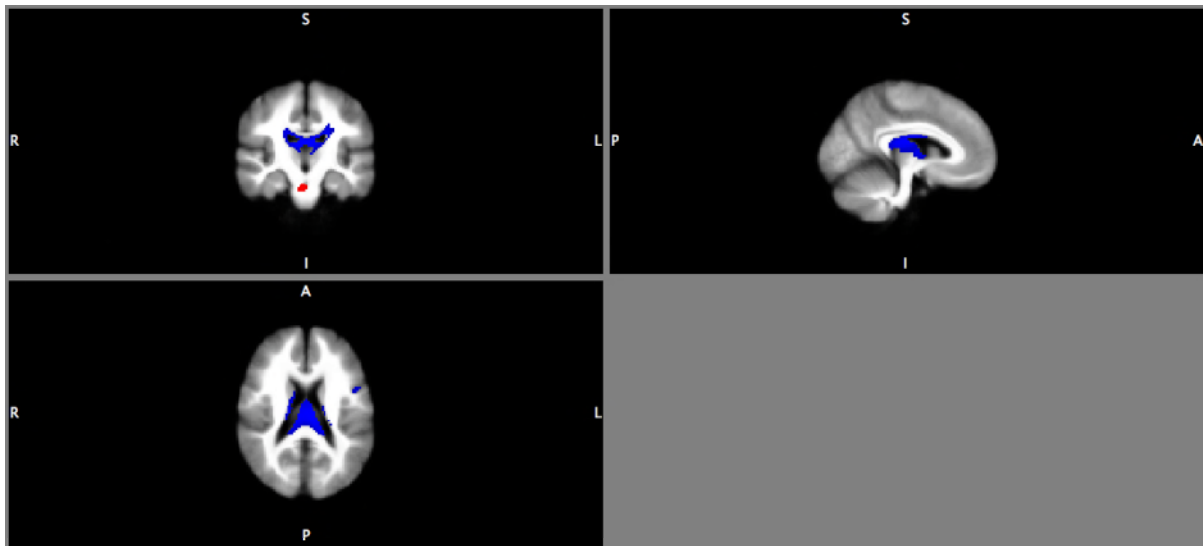
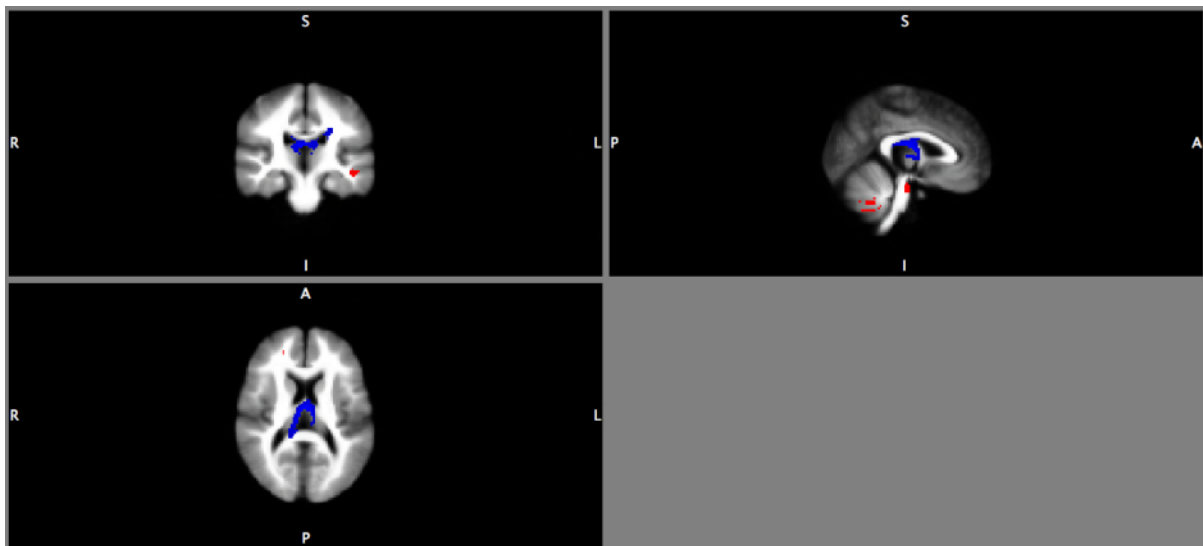


**Figure 2.** Signed differential mapping-generated FSL map of areas showing altered FA in patients with AN identified in main meta-analysis.



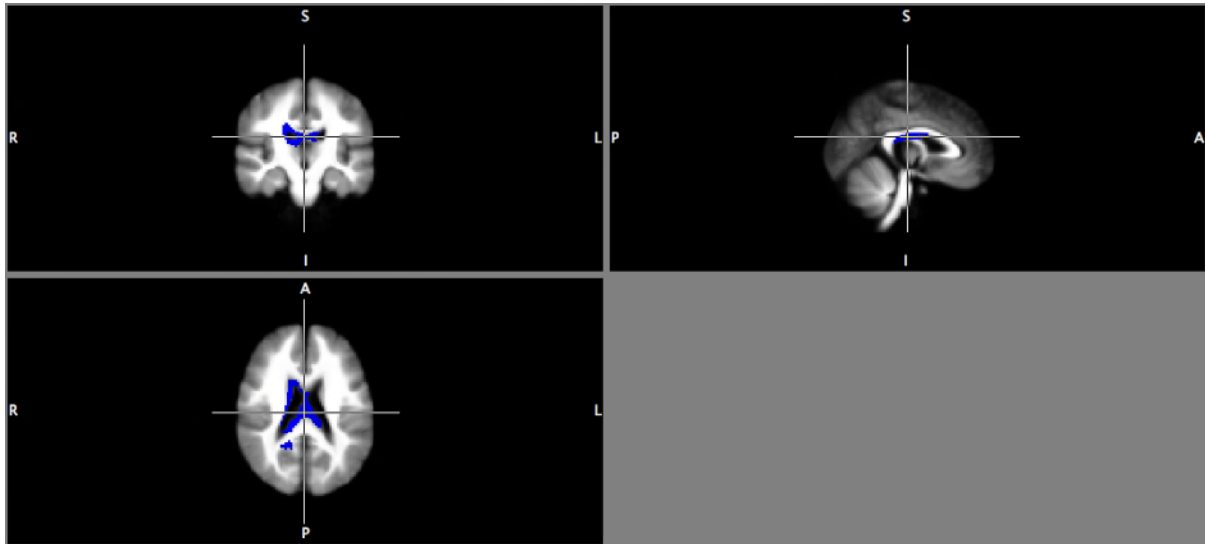
Significant regional differences in FA values in patients with AN compared to healthy controls. Clusters of decreased FA are marked in blue and increased FA are marked as red

**Figure 3.** Signed differential mapping-generated FSL map of areas showing altered FA in patients with acute AN.



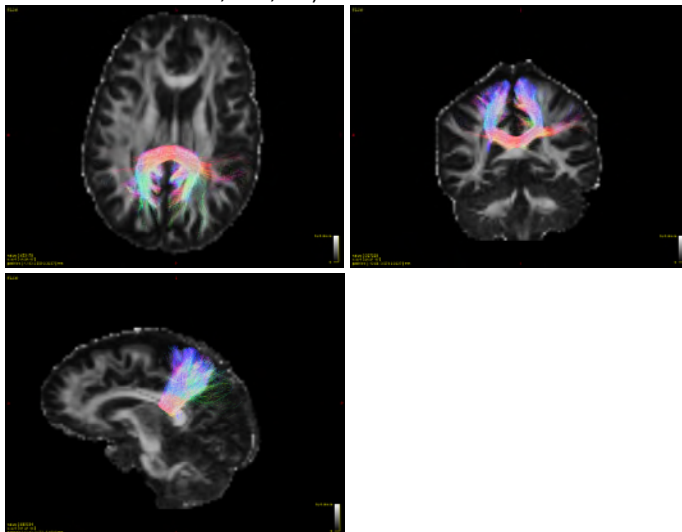
Significant regional differences in FA values in patients with acute AN compared to healthy controls. Clusters of decreased FA are marked in blue and increased FA are marked as red.

**Figure 4.** Signed differential mapping-generated FSL map of areas showing altered FA in adult patients with AN.



Significant regional differences in FA values in adult patients with AN compared to healthy controls. Clusters of decreased FA are marked in blue.

**Supplementary Figure 1.** Tractography images of main replicable cluster in the CC (MNI coordinates = 18,-56,28)



Three dimensional images showing WM tracts traversing a bounding box centred at  $x = 18$ ,  $y = -58$ ,  $z = 30$  (the most replicable coordinate from main analyses) was mapped with MRtrix in a single typical individual. Axial view (A), coronal view (B) and sagittal view (C).



**Supplementary figure 2:** Funnel plot demonstrating contribution of each study to the corpus callosum clusters.

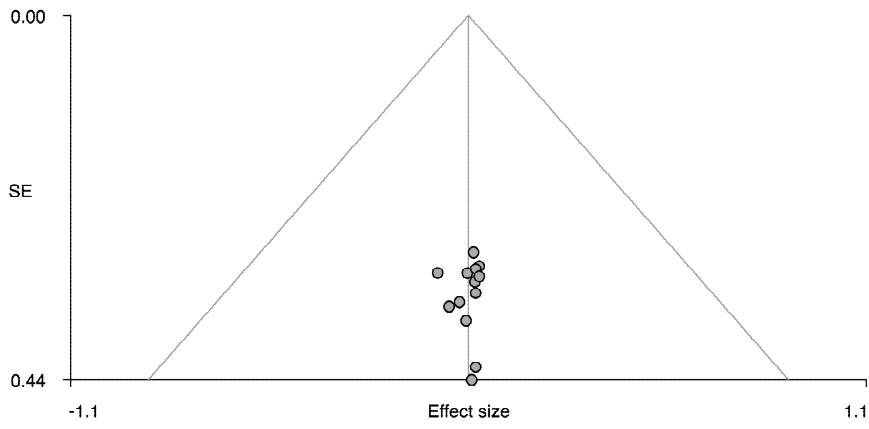


**Table 1.** Summary of demographics of studies included in meta-analysis conducted with patients with AN using whole-brain voxel-based analysis.

|                     | ED status | AN subtype | Age group   | Cases      | Controls   | Mean age_cases (sd) | Mean age_controls (sd) | BMI_cases (sd)    |
|---------------------|-----------|------------|-------------|------------|------------|---------------------|------------------------|-------------------|
| Kzlouski, 2011 (12) | Acute     | R and B/P  | Adult       | 16         | 17         | 23.9 (7)            | 25.1 (4)               | 16.5 (1)          |
| Frieling, 2012 (13) | Both      | R and B/P  | Adult       | 21         | 20         | 26.8 (6.9)          | 24.8 (2.6)             | 15.2 (1.4)        |
| Frank, 2013 (20)    | Acute     | R and B/P  | Adolescents | 19         | 22         | 15.4 (1.4)          | 14.8 (1.8)             | 16.2 (1.1)        |
| Yau, 2013 (17)      | Recovered | R          | Adult       | 12         | 10         | 28.7 (7.9)          | 26.7 (5.4)             | 21.2 (1.5)        |
| Via, 2014 (14)      | Acute     | R          | Adult       | 19         | 19         | 28.3 (9.5)          | 28.6 (8.6)             | 17.0 (1.1)        |
| Nagahara, 2014 (15) | Acute     | AN         | Adult       | 17         | 18         | 23.8 (6.6)          | 26.2 (5.6)             | 13.6 (1.3)        |
| Shott, 2015 (16)    | Recovered | R          | Adult       | 24         | 24         | 30.2 (8.1)          | 27.42 (6.3)            | 20.8 (2.4)        |
| Vogel, 2016 (21)    | Acute     | R and B/P  | Adolescents | 22         | 21         | 15.0 (1.6)          | 15.2 (1.3)             | 15.4 (1.1)        |
| Cha, 2016 (19)      | Acute     | AN         | Both        | 22         | 18         | 19.5 (2.4)          | 20.5 (2.9)             | 17.3 (1.2)        |
| Bang, 2017 (75)     | Recovered | AN         | Adult       | 21         | 21         | 27.6 (5.0)          | 26.1 (4.8)             | 20.5 (1.7)        |
| Gaudio, 2017 (23)   | Acute     | R          | Adolescents | 14         | 15         | 15.7 (1.6)          | 16.3 (1.5)             | 16.2 (1.2)        |
| Hu, 2017 (24)       | Acute     | R          | Both        | 8          | 14         | 17.6 (2.2)          | 19.1 (3.1)             | 14.3              |
| Olivo, 2017 (76)    | Acute     | EDNOS      | Adolescents | 12         | 24         | 15.3                | 14.1                   | 18.7              |
| <b>Total</b>        |           |            |             | <b>227</b> | <b>243</b> | <b>22.5 (5.0)</b>   | <b>21.9 (3.9)</b>      | <b>17.4 (1.4)</b> |

R: restricting; B/P: binge and purge

**Table 2.** Summary of technical imaging data and patient status at scanning time of studies included in meta-analysis conducted with patients with AN using whole-brain voxel-based analysis.

|                        | <b>MRI</b> | <b>Software</b>   | <b>p value</b>                          | <b>Patient status at scanning</b>   |
|------------------------|------------|-------------------|---|---|
| <b>Kazkiysju, 2011</b> | 3T         | SPM5 <sup>a</sup> | P < 0.05, corrected (FDR <sup>c</sup> ) | within one or two weeks of admission, no electrolyte abnormalities        |
| <b>Frieling, 2012</b>  | 3T         | SPM2              | P < 0.05, corrected (FDR)               | recovered: BMI of 18.5 and no ED behaviours one year; acute: AN diagnosis |
| <b>Frank, 2013</b>     | 3T         | SPM8              | p < 0.005 uncorrected                   | within two weeks of start of treatment no rehydration                     |
| <b>Yau, 2013</b>       | -          | FSL               | -                                       | Recovered: 12 months  |
| <b>Via, 2014</b>       | 1.5T       | FSL <sup>b</sup>  | p < 0.05, corrected (FWE <sup>d</sup> ) | at least one week of rehydration  |
| <b>Nagahara, 2014</b>  | 3T         | FSL               | p < 0.05, corrected                     | no signs of rehydration   |
| <b>Shott, 2015</b>     | -          | FSL               | p < 0.05, corrected (FWE)               | Recovered: 12 months, no ED behaviours                                    |
| <b>Vogel, 2016</b>     | 3T         | FSL/SPM           | P < 0.05, corrected                     | Weight at admission   |
| <b>Cha, 2016</b>       | 1.5T       | FSL               | -                                       | at least 24 hours of rehydration  |
| <b>Bang, 2016</b>      | 3T         | FSL               | p < 0.05, corrected (FWE)               | Recovered: 12 month   |
| <b>Gaudio, 2017</b>    | 1.5T       | FSL               | p < 0.05, corrected (FWE)               | duration of less than 6 months and scanned within a week of diagnosis     |
| <b>Hu, 2017</b>        | 3T         | SPM               | P < 0.05, corrected (FDR)               | at least one week of rehydration  |
| <b>Olivo, 2017</b>     | 3T         | FSL               | P < 0.05, corrected (FDR)               | upon diagnosis  |

<sup>a</sup>SPM: statistical parametric mapping; <sup>b</sup>FSL: FMRIB software library; <sup>c</sup>FDR: false discovery rate; <sup>d</sup>FWE: family-wise error rate

**Table 3.** Significant regional differences in FA values in patients with AN compared to healthy controls and results from Jackknife sensitivity analysis

| Region                                   | Maximum                    |           |                      | Cluster          |  | Jackknife sensitivity analysis |
|--|----------------------------|-----------|----------------------|------------------|--|--------------------------------|
|  | MNI coordinates<br>x, y, z | SDM value | Uncorrected <i>p</i> | Number of voxels | Breakdown (number of voxels)   |                                |
| <b>Clusters of decreased FA</b>          |                            |           |                      |                  |  |                                |
| Corpus callosum                          | -2,-18, 18                 | -1.954    | 0.000012696          | 2070             | Corpus callosum (945), thalamus (395), anterior thalamic projections (382), caudate nucleus (56), cortico spinal projections (77), pons (57) | 8/13                           |
| Corpus callosum                          | 18,-58,30                  | -1.770    | 0.000065684          | 262              | Corpus callosum (211), right precuneus (47), right cuneus (35)   | 10/13                          |
| Corpus callosum                          | -22,24,30                  | -1.335    | 0.001392961          | 91               | Corpus callosum (91)   | 10/13                          |
| Left superior longitudinal fasciculus II | -31,-34,36                 | -1.387    | 0.001008451          | 66               | Left superior longitudinal fasciculus II (66)  | 7/13                           |
| Left precentral gyrus, BA44              | -48,6,20                   | -1.304    | 0.001658022          | 31               | Left precentral gyrus BA44   | 9/13                           |
| <b>Clusters of increased FA</b>          |                            |           |                      |                  |  |                                |
| Right cortico-spinal projections         | 6,-16,-24                  | 1.008     | 0.000757337          | 69               | Right cortico spinal projections (61), right pons (29)   | 2/13                           |
| Right lingual gyrus, BA18                | 10,-86,-12                 | 1.006     | 0.000788093          | 31               | Right lingual gyrus  | 8/13                           |
| Left lingual gyrus, BA18                 | -28,-90,-14                | 1.001     | 0.000844777          | 20               | Left lingual gyrus   | 9/13                           |

less than 20 voxels are not represented in the breakdown of voxels

**Table 4.** Significant regional differences in FA values in subgroups of patients with AN (adult subgroup; acute subgroup)

| <b>Adult subgroup</b>            |                            |           |                      |                  |   |                                |  |
|----------------------------------|----------------------------|-----------|----------------------|------------------|---|--------------------------------|--|
| <b>Region</b>                    | <b>Maximum</b>             |           |                      | <b>Cluster</b>   |   | Jackknife sensitivity analysis |  |
|                                  | MNI coordinates<br>x, y, z | SDM value | Uncorrected <i>p</i> | Number of voxels | Breakdown (number of voxels)  |                                |  |
| Right caudate nucleus            | 16,2,24                    | -1.733    | 0.000043690          | 1387             | right caudate nucleus, corpus callosum  | 4/7                            |  |
| Corpus callosum                  | 18,-50,26                  | -1.483    | 0.000351667          | 196              | corpus callosum, cingulum, precuneus  | 6/7                            |  |
| <b>Acute subgroup</b>            |                            |           |                      |                  |   |                                |  |
| <b>Region</b>                    | <b>Maximum</b>             |           |                      | <b>Cluster</b>   |   | Jackknife sensitivity analysis |  |
|                                  | MNI coordinates<br>x, y, z | SDM value | Uncorrected <i>p</i> | Number of voxels | Breakdown (number of voxels)  |                                |  |
| Clusters of decreased FA         |                            |           |                      |                  |   |                                |  |
| Undefined                        | 2,-14,14                   | -1.935    | 0.000019729          | 1055             | corpus callosum, thalamus, anterior thalamic projections, left pons, left cortico-spinal projections, right caudate nucleus, left SLF | 6/9                            |  |
| Corpus callosum                  | -22,24,30                  | -1.447    | 0.000822186          | 203              | Corpus callosum   | 7/9                            |  |
| Left precentral gyrus, BA44      | -48,6,20                   | -1.401    | 0.001111686          | 77               | Left inferior frontal gyrus (opercular part), left precentral gyrus   | 7/9                            |  |
| Left pons                        | -22,-14,-8                 | -1.285    | 0.002091289          | 43               | Left pons, left optic radiations  | 7/9                            |  |
| Right median network, cingulum   | 16,-56,28                  | -1.285    | 0.002850354          | 20               | Corpus callosum, cingulum   | 7/9                            |  |
| Clusters of increased FA         |                            |           |                      |                  |   |                                |  |
| Undefined                        | -2,-52,-42                 | 1.027     | 0.002499163          | 216              | Cerebellum  | 7/9                            |  |
| Right cortico-spinal projections | 8,-18,-28                  | 1.065     | 0.001279950          | 85               | Cortico spinal projections, pons  | 4/9                            |  |
| Corpus callosum                  | -46,-22,-8                 | 1.030     | 0.002317071          | 57               |   |                                |  |
| Corpus callosum                  | -20,44,18                  | 1.030     | 0.002317071          | 50               |   | 7/9                            |  |

|  |             |       |             |    |     |
|--|-------------|-------|-------------|----|-----|
| Corpus callosum                        | 16,52,-8    | 1.030 | 0.002317071 | 46 | 5/9 |
| BA 18                                  | 8,-86,-14   | 1.062 | 0.001305223 | 39 |     |
| Left lenticular nucleus, putamen, BA48 | -28,10,0    | 1.065 | 0.001258790 | 30 | 8/9 |
| Left lingual gyrus, BA18               | -28,-88,-16 | 1.061 | 0.001336217 | 26 | 6/9 |
| Right arcuate network, post. Segment   | 46,-36,10   | 1.062 | 0.001305223 | 25 | 8/9 |
| Left superior temporal gyrus, BA48     | -54,-16,4   | 1.027 | 0.002499163 | 25 | 7/9 |

---